

# 3D U-Net for brain stroke lesion segmentation on ISLES 2018 dataset

Azhar Tursynova  
Department of Artificial Intelligence and Big Data  
al-Farabi Kazakh National University  
Almaty, Kazakhstan  
azhar.tursynova1@gmail.com

Batyrcan Omarov  
al-Farabi Kazakh National University,  
Suleiman Demirel University  
Almaty, Kazakhstan  
batyahan@gmail.com

**Abstract** – Brain stroke is one of the global problems today. An image such as a CT scan helps to visually see the whole picture of the brain. Segmentation of the affected brain regions requires a qualified specialist. However, manual segmentation requires a lot of time and a good expert. The role and support of trained neural networks for segmentation tasks is considered as one of the best assistants. Among the neural network models, the models based on U-Net are recognized as the leading ones. The U-Net architecture can work with a small number of datasets and is considered advanced for the segmentation method. In this paper, we use the classical U-Net architecture for the experiment. As datasets, we use 3D computed tomography images of the brain taken from ISLES 2018 the public domain. Using the classical U-Net architecture, we found that U-Net is considered the best architecture for segmentation methods. This study presents experiment results of 3D U-Net model for brain stroke lesion segmentation, and gives future perspectives for researchers who is going to segment brain strokes and create modified U-Net model for improvement. The developed model is useful for brain stroke segmentation when there is little number of images for train and testing the model.

**Keywords** – Deep Learning, U-Net, brain stroke, computed tomography, segmentation

## I. INTRODUCTION

Inadequate blood supply to the brain causes a stroke. As a result, the brain is deprived of oxygen and vital nutrients, causing brain cells to die. A stroke can be either ischemic, which is caused by a clogged or leaking artery, or hemorrhagic, which is caused by the rupture of a blood vessel. Compared to hemorrhagic stroke, which accounts for about 15% of strokes, ischemic stroke is the most common type, accounting for about 87% of strokes [1].

To diagnose a disease accurately, a visual examination of the brain and its vessels is necessary. To date, the most common single type of imaging is noncontrast computed tomography (CT) because it is rapid and widely available. When read correctly, computed tomography of the brain can assist identify hemorrhagic stroke (intracerebral or subarachnoid hemorrhage) with more than 95% accuracy. When ischemic alterations are visible on a CT scan of the head, it can assist detect a large stroke in roughly two-thirds of instances, but it is highly insensitive for diagnosing a little stroke; hence, a right scan does not confirm or rule out ischemia in the minor stroke scenario. The method of choice for complicated diagnosis of minor stroke in instances when the impairment is extremely mild is magnetic resonance imaging (MRI), which has greater spatial resolution for identifying cerebral ischemia in

transient ischemic attack or mild ischemic stroke [2]. Manual segmentation is the conventional technique of evaluating stroke lesions. It entails manually tracing the stroke regions on all neighboring portions that have been identified as damaged. This manual segmentation takes a long time to complete and can be altered at any moment. Another drawback of these interventions is that they rely on subjective assessments, which makes it more likely that various observers may come to different conclusions regarding the presence or absence of lesions, or that the same observer would come to different findings in different cases. As a result, a computerized automated system for assessing stroke MRI pictures as they are collected might be very useful in clinical practice [3]. The science of computer vision has advanced significantly in recent years because to Deep Learning. Despite the fact that researchers have found many ways to solve many visual problems, especially in biomedical image processing, the U-Net convolutional neural network is fast and accurate for image segmentation. In this article, we also use the U-Net convolutional network model and also use the dataset ISLES 2018 3D CT images of the brain as an experiment.

The reminder of this study is as following: Next section reviews related works. Section III describes ISLES 2018 dataset that applied in current research. Section IV explains the 3D-UNet model that used to stroke lesion segmentation. Section V presents the obtained results, and in the end, we conclude our study.

## II. LITERATURE REVIEW

For the segmentation of medical images, the classical U-Net architecture has been well proven. Many scientists and researchers have made various discoveries in the field of medicine. For example, in order to collect information about the boundaries of the disease, the evolution, the number and the size of the studied area of the gastrointestinal tract, as well as to stimulate further research, the scientists in [4] demonstrate the use of the classical U-Net architecture in their work. Based on the U-Net, the authors of [5] also proposed the use of a recurrent convolutional neural network (RCNN) and a recurrent residual convolutional neural network (RRCNN). These models were tested on datasets such as retinal blood vessels, skin cancer, and affected lungs. The developed models assisted the residual units in learning the architecture, provided a better representation of objects for the collection of objects with repeated residual convolutional layers, moreover, they allowed the use of the same number of network parameters as in a conventional

U-Net. The ladder-net model, which is a concatenation of multiple U-Nets, was created by researchers in [6]. This model has multiple pairs of encoder-decoder branches and has a connection passage at each level between each pair of adjacent branches. The ladder-net model was tested on two datasets for segmenting blood vessels in retinal images. Another example of using U-Net was seen in [7] where it was used for segmentation of biventricular heart volume estimation. The Shape-U-Net architecture created emphasizes model interpretability and reliability. For the segmentation of MRI images of the brain, the researchers in [8] provided a SAU -net model with divided attention and access paths, where one of the main tasks was the preparation and fine-tuning with Free Surfer tags, which finally resulted in effective training. The implementation of this task allows the use of heterogeneous neuroimaging data in training without additional annotations in the manual. As an experiment, 9 datasets were used for evaluation. The SAU -network model is resistant to neuroanatomical variability and provides instant access to accurate neuroimaging biomarkers. The lightweight U-Net network proposed in [9] has also been used for microscopic image analysis tasks. The model is designed for nuclei segmentation and the computations require few resources. To improve the accuracy of breast mass segmentation on digital images of breast tomosynthesis DBT, researchers proposed their own algorithms for the U-Net architecture in [10]. Another model based on U-Net for semantic segmentation of breast ultrasound images in [11]. The innovation presented was related to training, where it was proposed to apply an extended approach. As a result, the output map retains the details of the texture and features of the edges of breast tumors. One of the interesting discoveries [12] with the use of U-Net was made in creating an algorithm for segmentation of mesenchymal stem cells (MSCs) for objective, fast and non-invasive evaluation of the cells. This architecture used 71 phase contrast micrographs with 472 cells in training. In [13], a right ventricle segmentation method based on U-Net with improvements was also proposed. The developed method allows to apply datasets in the training stages without losing information about the right ventricle. As you can see, the application area of U-Net architecture is widely used in medicine. The following application example is described in the article [14], where U-Net was used to segment plasmodia on images of thin blood smears, and the standard error, Huber loss, and binary cross entropy were also compared. In the article [15], the authors proposed a multiscale pixel-level U-Net model using 224 histological images obtained during radical prostatectomy in 20 patients to evaluate histological images according to Gleason, in the treatment of patients with prostate cancer. The use of U-Net for the detection and isolation of brain tumors present on MRI has not been spared. The model in [16] is compact, the time required is minimal, and the accuracy of the prediction is maintained. Adadelta was used as an optimizer, as well as a smaller number of layers and convolutional filters. The use of combined U-Net architectures was observed in [17], where the Double U-Net method was developed to improve the performance of the classical U-Net. In this work, different imaging techniques were used such as colonoscopy, dermatoscopy and microscopy. The dual U-Net is far superior to the classical version of U-Net and provides more accurate segmentation masks. It has proven that it

can be used in medical image segmentation as a reliable basis. A group of researchers in [18] conducted a study and created a universal U-Net model for various tasks that requires adding a minimal number of parameters and is controlled for each task. There is a possibility that this universal promising model can extend its task domain independently of different organs and visualization methods. The developed model can compete equally with other models that use only 1% of parameters.

### III. DATA

The 3D U-Net model was tested on the free ISLES 2018 datasets, which are publicly available at the link [19]. This ISLES 2018 database is available under the Open Database license, and the full text can be found at [20].

Any rights to individual database contents are licensed according to the Database Content License. For a summary worth reading, see [21]. The ISLES 2018 dataset consists of training and testing data, with the training data containing data from 63 patients and the testing data containing data from 40 patients. The created methods are evaluated using a research dataset that contains 40 cases of stroke. Some patients have 2 records to cover the focus of stroke. These are non-overlapping or partially overlapping areas of the brain. The plates for the patient are labeled accordingly with the characters " A " and " B " for 1 and 2 plates (e.g., 39\_A = case 60 ; 39\_B = case 61). The image format is .nii, the uncompressed Neuroimaging Information Technology Initiative (NifTI) format. There are also naming conventions: SMIR.your\_description.#####.nii. Where # # # denotes the corresponding SMIR identifier that allows the system to correlate the creator's segmentation with the correct ground truth. The results of the test provide a brief summary of individual estimates that can be used to evaluate layouts. The results in the individual case are not accessible to the researcher in order to minimize the overhead in cases where the methods are literally configured for a set of test data. The data for the training phase is divided into two sections: Training and Validation. Fig. 1 shows an illustrative example of the ISLES 2018 dataset image

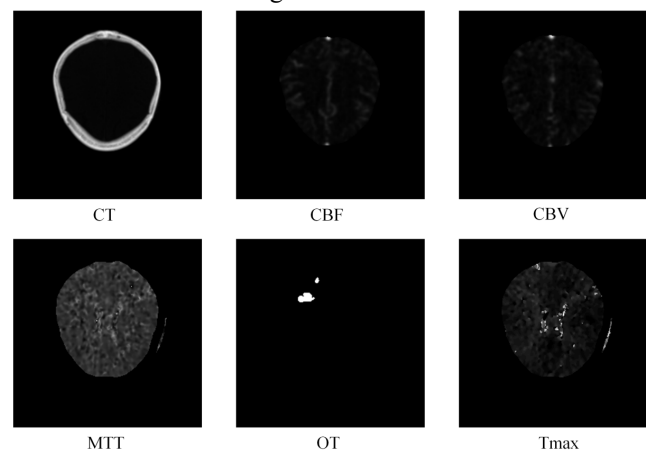


Fig. 1. Example of ISLES 2018 images (computed tomography (CT), cerebral blood flow (CBF), cerebral blood volume (CBV), mean transit time (MTT), segmentation image (OT), tissue residue function (Tmax))

After the validation phase is completed, the model is tested on a test set, the results of which are then sent to [22] for verification to obtain results.

## IV. METHOD

In many visual tasks, especially in the processing of biomedical images, the desired result must include localization, i.e., each pixel is expected to have a class label associated with it. In this respect, among convolutional neural networks, the U-Net architecture can be distinguished as one of the most important. It is the U-Net that can provide the best segmentation for medical images while having a small amount of data.

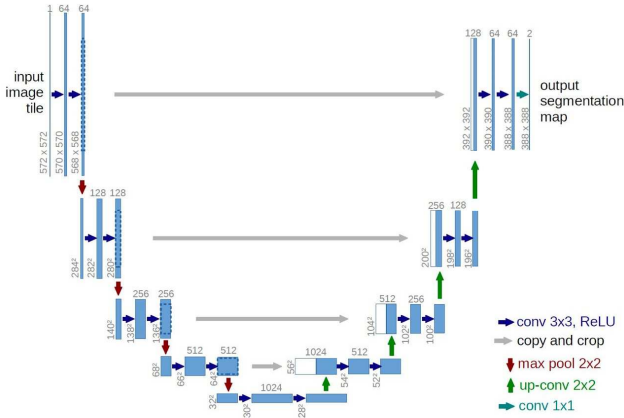


Fig. 2. U-Net architecture

The U-Net architecture, as shown in Fig. 2, has a U-shape with the encoding path on the left and the decoding path on the right. The encoding path, or in other words, the reduction, is generated by the repeated use of a 3x3 convolution, each followed by the ReLU function and the 2x2 max-union operation with a step of 2 for downsampling. At each step of downsampling, the number of active channels doubles. This strengthens the context with support for small-scale object mapping. The decoding path, or expansion in other words, consists of sampling the object map, followed by the 2x2 convolution which halves the number of object channels, grouping with a clipped object map from the compression path, and the 3x3 convolution, followed by the ReLU footsteps. The increase of the object volume is done for the ratio of the same volume as the block connected to the left [23]. There are different sizes of data, starting from 1D, 2D-which is common among researchers and further, in our model we use 3D data.

### A. Evaluation criteria

There are criteria for evaluating neural network models, such as Dice, accuracy, recall, and the Jaccard index [24-26].

Dice score can be expressed in terms of TP (true positives), FP (false positives) and FN (false negatives) as follows: Simply put, Dice Coefficient is twice the overlap area divided by the total number of pixels in both images. Formula (1) shows the dice calculation.

$$Dice = \frac{2 \times TP}{(TP + FP) + (TP + FN)} \quad (1)$$

Precision is the ratio between true positives and all positives. Mathematically represented in formula (2):

$$Precision = \frac{TP}{TP + FP} \quad (2)$$

Recall is an indicator that the neural model is correctly determining the true positive outcomes. Mathematically represented in formula (3):

$$Recall = \frac{TP}{TP + FN} \quad (3)$$

The intersection over union (IoU) or Jaccard index is a method for quantifying the percentage overlap between the target mask and model prediction results. This metric is closely related to the dice coefficient, which is often used as a function of losses during training. Formula (4) calculates the Jaccard index.

$$IoU = \frac{target \cap prediction}{target \cup prediction} \quad (4)$$

## V. EXPERIMENT RESULTS

Using the three-dimensional CT images of the 2018 ISLES dataset, we performed an experiment based on the classical U-Net architecture for segmentation of brain stroke images. During the training, the results of train loss and validation loss, line graph, which is shown in Fig. 3, were obtained. The training was achieved and completed with 146 epochs.

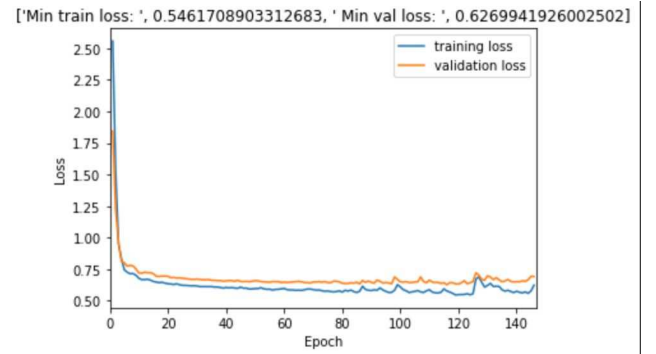


Fig. 3. Train and validation loss (146 epochs)

Table 1 shows the results of the average dice, average precision, average recall, and average jaccard for the training level, as well as the test results of the trained classical 3D U-Net model.

TABLE 1. TRAINING AND TESTING RESULTS OF CLASSICAL 3D U-NET MODEL

Evaluation criteria	Training results	Testing results
Average dice	0.39	0.35
Average recall	0.33	0.48
Average precision	0.99	0.35
Average Jaccard	0.28	0.24

Fig. 4 shows three examples of the segmented original images on the right and the predicted images on the left. From the figure, it can be seen that the classical U-grid model we used in the experiment accurately determines the affected area on 3D images CT.

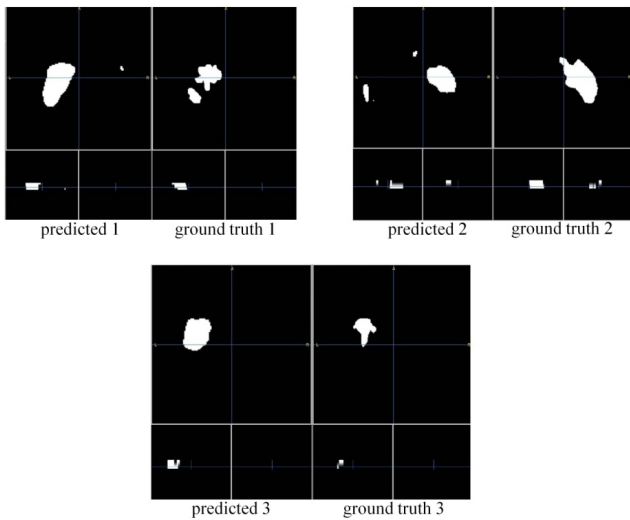


Fig. 4. Train and validation loss (146 epochs)

## VI. CONCLUSION

In summary, the process of segmenting the affected foci from a stroke in the brain area requires precise determination in automation. It is recognized that convolutional neural networks are capable of performing this task no worse than a human expert performs. In addition, for working with small amount of data and segmentation, the U-Net architecture has shown its best side. However, based on the experiments performed, it has been shown that the classical U-Net model needs additional modifications for more accurate detection and determination of the stroke affected area for segmentation. Thus, we have identified the main model for us and in future, we will improve and add to this model for high accuracy of dice, precision and recall.

## REFERENCES

- [1] D. Kuriakose, and Z. Xiao, "Pathophysiology and treatment of stroke: present status and future perspectives," *International journal of molecular sciences*, vol. 21, pp. 7609, 2020.
- [2] T. D. Musuka, S. B. Wilton, M. Traboulsi, and M. D. Hill, "Diagnosis and management of acute ischemic stroke: speed is critical," *Cmaj*, vol. 187, pp. 887-893, 2015.
- [3] Y. Kabir, M. Dojat, B. Scherrer, F. Forbes, and C. Garbay, "Multimodal MRI segmentation of ischemic stroke lesions," in *29th Annual International Conference of the IEEE Engineering in Medicine and Biology Society*, pp. 1595-1598, 2007.
- [4] D. Jha, S. Ali, K. Emanuelsen, S. A. Hicks, V. Thambawita et al., "Kvasir-instrument: diagnostic and therapeutic tool segmentation dataset in gastrointestinal endoscopy," in *International Conference on Multimedia Modeling*, pp. 218-229, 2021.
- [5] M. Z. Alom, M. Hasan, C. Yakopcic, T. M. Taha, and V. K. Asari, "Recurrent residual convolutional neural network based on U-Net (R2U-Net) for medical image segmentation," 2018.
- [6] J. Zhuang, "LadderNet: multi-path networks based on U-Net for medical image segmentation," *arXiv preprint arXiv:1810.07810*, 2018.
- [7] J. Sun, F. Darbehani, M. Zaidi, and B. Wang, "Saunet: shape attentive U-Net for interpretable medical image segmentation," in *International Conference on Medical Image Computing and Computer-Assisted Intervention*, pp. 797-806, 2020.

- [8] M. Lee, J. Kim, EY R. Kim, H. G. Kim, S. W. Oh et al., "Split-Attention U-Net: a fully convolutional network for robust multi-label segmentation from brain MRI," *Brain Sciences*, vol. 10, pp. 974, 2020.
- [9] F. Long, "Microscopy cell nuclei segmentation with enhanced U-Net," *BMC bioinformatics*, vol. 21, pp. 1-12, 2020.
- [10] X. Lai, W. Yang, and R. Li, "DBT masses automatic segmentation using U-Net neural networks," *Computational and mathematical methods in medicine*, vol. 2020, 2020.
- [11] Y. Guo, X. Duan, C. Wang, and H. Guo, "Segmentation and recognition of breast ultrasound images based on an expanded U-Net," *Plos one*, vol. 16, pp. e0253202, 2021.
- [12] S. M. Mota, R. E. Rogers, A. W. Haskell, E. P. McNeill, R. Kaunas et al., "U-Net based image segmentation of mesenchymal stem cells," in *Imaging, Manipulation, and Analysis of Biomolecules, Cells, and Tissues XIX*, pp. 116470V, 2021.
- [13] Y. Miao, C. X. Shen, W. L. Shi, K. Zhang, Z. G. Jiang et al., "A right ventricle segmentation method based on U-Net with weighted convolution and dense connection," in *Proceedings of the 2020 2nd International Conference on Intelligent Medicine and Image Processing*, pp. 40-46, 2020.
- [14] J. B. Abraham, "Malaria parasite segmentation using U-Net: comparative study of loss functions," *Communications in Science and Technology*, vol. 4, pp. 57-62, 2019.
- [15] J. Li, K. V. Sarma, K. C. Ho, A. Gertych, B. S. Knudsen et al., "A multi-scale U-Net for semantic segmentation of histological images from radical prostatectomies," in *AMIA Annual Symposium Proceedings*, pp. 1140, 2017.
- [16] K. Gonzalez, M. Camp, and M. Zhang, "3D brain tumor segmentation: narrow UNet CNN," in *IEEE MIT URTC (Undergraduate Research Technology Conference)*, 2018.
- [17] D. Jha, M. A. Riegler, D. Johansen, P. Halvorsen, and H. D. Johansen, "DoubleU-Net: a deep convolutional neural network for medical image segmentation," in *2020 IEEE 33rd International symposium on computer-based medical systems (CBMS)*, pp. 558-564, 2020.
- [18] C. Huang, H. Han, Q. Yao, S. Zhu, and S. K. Zhou, "3D U<sup>2</sup>-Net: a 3D universal U-Net for multi-domain medical image segmentation," in *International Conference on Medical Image Computing and Computer-Assisted Intervention*, pp. 291-299, 2019.
- [19] The ISLES Challenge 2018 website. [Online]. Available: <https://www.smir.ch/ISLES/Start2018>
- [20] The open data commons website. [Online]. Available: <https://opendatacommons.org/licenses/d-bcl/>
- [21] The open data commons website. [Online]. Available: <http://opendatacommons.org/licenses/o-dbl/summary/>
- [22] The smir website. [Online]. Available: <https://www.smir.ch/ISLES/Evaluation?challengeType=ISLES2018Testing>
- [23] The towards data science website. [Online]. Available: <https://towardsdatascience.com/paper-summary-U-Net-convolutional-networks-for-biomedical-image-segmentation-13f4851ccc5e>
- [24] Omarov, B., Saparkhojayev, N., Shekerbekova, S., Akhmetova, O., Sakypbekova, M. et al. (2022). Artificial Intelligence in Medicine: Real Time Electronic Stethoscope for Heart Diseases Detection. *CMC-Computers, Materials & Continua*, 70(2), 2815-2833.
- [25] Murzamadiyeva, M., Ivashov, A., Omarov, B., Omarov, B., Kendzhayeva, B., & Abdrakhmanov, R. (2021, January). Development of a System for Ensuring Humidity in Sport Complexes. In 2021 11th International Conference on Cloud Computing, Data Science & Engineering (Confluence) (pp. 530-535). IEEE.
- [26] Kendzhaeva, B., Omarov, B., Abdiyeva, G., Anarbayev, A., Dauletbek, Y., & Omarov, B. (2020, December). Providing Safety for Citizens and Tourists in Cities: A System for Detecting Anomalous Sounds. In International Conference on Advanced Informatics for Computing Research (pp. 264-273). Springer, Singapore.